

## Structural Studies by Electron Microscopy: High-Resolution Observations on $\beta$ - $\text{ZrO}_2 \cdot 12\text{Nb}_2\text{O}_5$

J. G. ALLPRESS

*Division of Tribophysics, C.S.I.R.O., University of Melbourne, Australia*

S. IJIMA\*

*Department of Physics, Arizona State University, U.S.A.*

R. S. ROTH

*Institute for Materials Research, National Bureau of Standards, U.S.A.*

N. C. STEPHENSON

*School of Chemistry, University of New South Wales, Australia*

Received August 21, 1972

Reliable idealized structures for the  $\beta$  and  $\gamma$  forms of  $\text{ZrO}_2 \cdot 12\text{Nb}_2\text{O}_5$  have been deduced following the observation of lattice images, recorded at a resolution of about 0.3 nm, from crystals oriented with their short  $b$  axes parallel to the incident electron beam. The structure of the  $\beta$  form is confirmed by preliminary results from single crystal X-ray studies. The present observations are compared with previous work on these phases.

A previous communication (1) described an attempt to characterize the polymorphs of  $\text{ZrO}_2 \cdot 12\text{Nb}_2\text{O}_5$  on the basis of electron diffraction and medium resolution (ca. 0.8 nm) microscopy. By these means, it was established that three forms of this material existed, and that the  $\alpha$  polymorph was isostructural with  $\text{TiNb}_{24}\text{O}_{62}$  (2). The electron optical evidence showed that the  $\beta$  and  $\gamma$  forms were also block structures belonging to the family related to high-temperature  $\text{Nb}_2\text{O}_5$  (3), and that they were both derived from a common subcell. Several possible structures for this subcell were suggested, and idealized models for the  $\beta$  and  $\gamma$  polymorphs were postulated.

More recently, the  $\beta$  phase has been the subject of a single-crystal X-ray diffraction study (4), which, because of the size of the unit cell (348 atoms), has proved to be extremely tedious, in spite of the existence of the electron optical results and the postulated model structure.

The same sample has now been examined in an electron microscope at high resolution (ca.

0.3 nm), and the results show sufficient detail to allow an idealized model to be proposed with confidence. The X-ray data is being re-examined using this model as a basis, and the preliminary results indicate that the model must be substantially correct.

### Experimental

A sample of  $\text{ZrO}_2 \cdot 12\text{Nb}_2\text{O}_5$  which had been annealed at 1640 K for 161 hr was selected for the present work. It was previously shown (1) to be predominantly the  $\beta$  polymorph, with a small proportion of the  $\gamma$  phase included.

The electron microscopy was carried out on a slightly modified JEM 100B instrument (5). Thin fracture fragments from the sample were prepared by grinding, and distributed randomly on carbon-coated specimen grids. In the present experiments, a perforated carbon film was used to support the fragments, and observations were restricted to thin sections of the fragments which projected over a hole in the film, and which were oriented so that their  $b$  axes were exactly parallel to the incident electron beam. Thus, two-

\* On leave from Research Institute for Scientific Measurements, Tohoku University, Sendai, Japan.

dimensional lattice images were obtained without interference from the phase contrast due to the carbon film. The primary magnification of the instrument was  $420,000\times$ , and features within the images which were spaced at about 0.3 nm or more were distinguishable by eye, with the aid of a  $10\times$  binocular, focused on the fluorescent screen of the electron microscope. The higher resolution of the instrument, and the use of perforated carbon supporting films, are the only major experimental differences between this and the previous work (1). Experience with related materials (5) has shown that the optimum defocus required to give contrast in the image which is interpretable directly in terms of structure is somewhat less than 100 nm under-focus from the Gaussian image plane.

A small single crystal for the X-ray studies was

selected from the same sample. Great difficulty was experienced in finding a crystal which was free from twins and domains of the  $\gamma$  form. A total of 2948  $h0l$  reflections were scanned, using an automatic diffractometer. The dimensions of the monoclinic unit cell were found to be  $a = 3.696$  nm,  $b = 0.3830$  nm,  $c = 3.549$  nm,  $\beta = 116.53^\circ$ , only slightly different from the less accurate estimate obtained from electron diffraction patterns (1).

## Results

### *Electron Microscopy*

A two-dimensional lattice image, recorded after tilting a crystal until the electron beam was incident parallel to  $b$ , is reproduced in Fig. 1. The image contrast within this area is represented

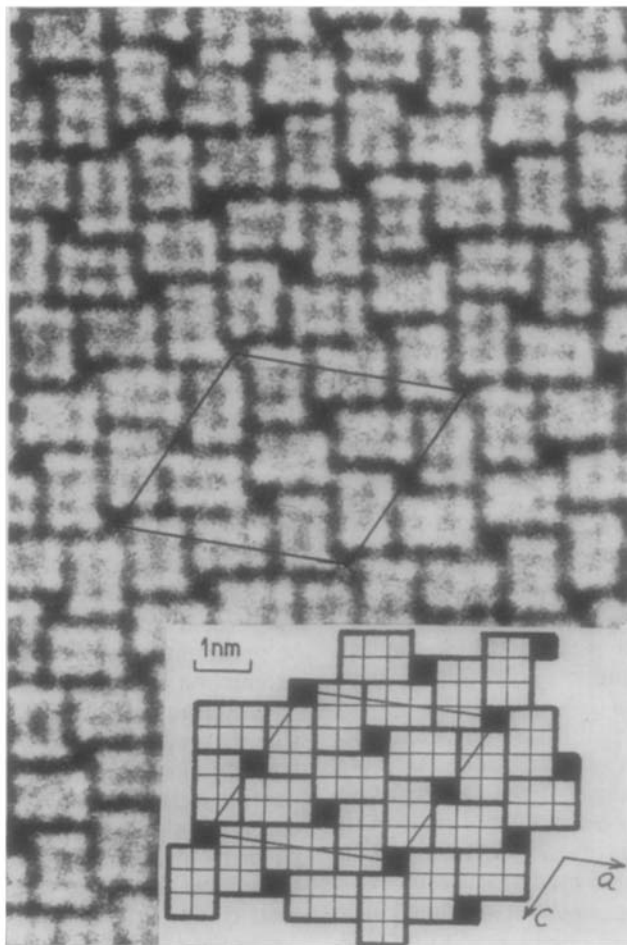


FIG. 1. Lattice image from a thin fragment of  $\beta\text{-ZrO}_2 \cdot 12\text{Nb}_2\text{O}_5$ , viewed down the short  $b$  axis. The unit cell is outlined. The inset shows a schematic representation of the contrast.

ideally in the inset. It consists of a square array of dark squares, surrounded by rectangles, each of which contains a double row of 3 white dots. The contrast within the rectangles is characteristic of that expected from  $4 \times 3$  blocks of corner-shared octahedra, each of which contains six empty tunnels. The dark lines surrounding each rectangle represent the crystallographic shear planes, where adjacent blocks are joined by sharing octahedral edges. Exactly similar contrast was observed in images from fragments of  $\text{Ti}_2\text{Nb}_{10}\text{O}_{29}$  (6), which also contains  $4 \times 3$  blocks. The geometry of the dark squares is correct for sites occupied by metal atoms in tetrahedral, rather than octahedral coordination.

An idealized model of the structure derived from the lattice image is shown in Fig. 2. Its monoclinic unit cell has primitive symmetry, in accord with the earlier electron diffraction data (1), and the disposition of  $4 \times 3$  blocks of octahedra and tetrahedral sites (black circles) is consistent with the contrast in Fig. 1. There are four formula units of  $\text{ZrNb}_2\text{O}_6$  in each unit cell, and 174 atoms in the asymmetric unit.

#### X-ray Diffraction

The structure shown in Fig. 2 was consistent with the Patterson function  $P(u,w)$  on (010). The appropriate minimum function was contoured from Patterson projections and the positions of all the metal atoms in the asymmetric unit were thereby determined. Some of the oxygen atoms

appeared in the minimum function, and the positions of the remainder were calculated from idealized coordinates by taking into account the known distortions which occur in octahedra which share edges along crystallographic shear planes. The initial set of calculated structure factors gave a reliability index ( $R$ ) of 0.44, but two cycles of least-squares refinement of metal atom positional parameters and isotropic thermal parameters reduced this value to 0.19. Extensive least-squares refinement cycles of atomic parameters are now being carried out using an IBM 360/50 computer.

#### Discussion

A simplified representation of the structure in Fig. 2, in which each block of octahedra is represented by a rectangle, is shown on the left of Fig. 3a. Defects of two different kinds were observed previously in this material (1), and both are readily accounted for by the model in Fig. 3a. The defect labelled Q may be regarded as an antiphase boundary; its presence displaces the unit cell by an amount equal to  $c/2$ . It also produces a microdomain of the  $\gamma$  form of  $\text{ZrO}_2 \cdot 12\text{Nb}_2\text{O}_5$ , which is orthorhombic (pseudo-tetragonal). The defect labelled P corresponds to the intergrowth of a slab of the  $\text{M}_{13}\text{O}_{33}$  ( $M = \text{metal}$ ) structure, and it alters the composition of the material in the direction of  $\text{Nb}_2\text{O}_5$ .

The differences between the idealized structure

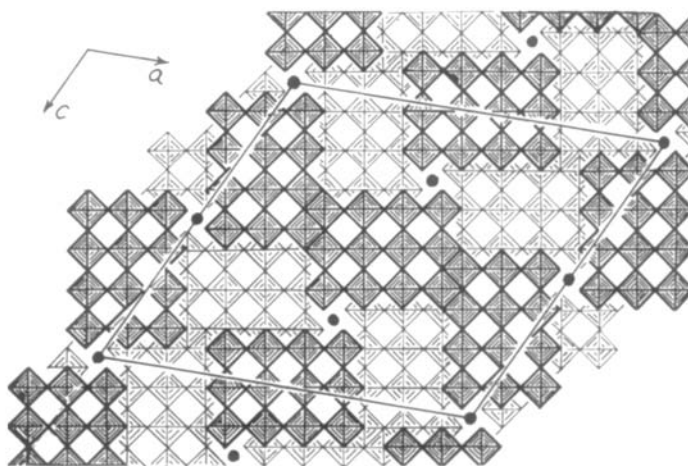


FIG. 2. Idealized model of the structure of  $\beta\text{-ZrO}_2 \cdot 12\text{Nb}_2\text{O}_5$ , derived from the lattice image in Fig. 1. Each hatched square represents an octahedron, centred on a metal atom, and with oxygen at the corners. The octahedra form blocks of  $4 \times 3$  by sharing corners, and adjacent blocks are joined by edge-sharing. Metal atoms within octahedra which are drawn light and dark lie at  $y = 0$  and  $y = \frac{1}{2}$  respectively. Filled circles represent metal atoms in tetrahedral coordination.

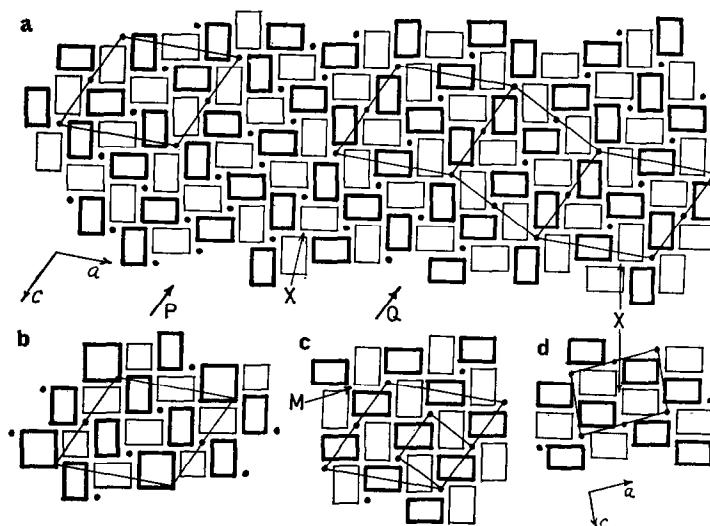


FIG. 3. a. Simplified representation of the structure of  $\beta\text{-ZrO}_2 \cdot 12\text{Nb}_2\text{O}_5$ , showing the incorporation of defects at P and Q. Each  $4 \times 3$  block of octahedra is shown as a rectangle. The defect P is a slab of composition  $\text{M}_{13}\text{O}_{33}$ , and Q is an antiphase boundary, which produces a slab of the  $\gamma$  polymorph. Unit cells of the monoclinic  $\beta$  phase and of the orthorhombic (pseudotetragonal)  $\gamma$  phase (near Q) are outlined. b. Previous proposed structure for the  $\beta$  phase (1). c. Tetragonal subcell, from which the superlattice is derived by the elimination of junctions between blocks of the type marked M. d. The structure of  $\alpha\text{-ZrO}_2 \cdot 12\text{Nb}_2\text{O}_5$ .

based on high-resolution lattice images (Figs. 2, 3a) and that which was proposed previously (Fig. 3b) are such that the objections to the earlier model (1) are overcome. The model in Fig. 3b was derived from a tetragonal subcell (Fig. 3c), by altering some of the block sizes to  $4 \times 4$  and  $3 \times 3$ , and thereby eliminating one tetrahedral site per unit cell. The reason for doing this was that the medium resolution lattice images (1) appeared to indicate that the monoclinic superlattice was caused by a periodic modification of tetrahedral sites. The high-resolution results show clearly that this conclusion was incorrect, and that the real structure is even more closely related to that of the subcell (Fig. 3b) than the previous model. The arrangement of tetrahedral sites is exactly the same, and all the blocks remain the same size, but the orientations of half of them are altered by  $90^\circ$ .

The question which immediately arises is "why is the structure in Figs. 2, 3a preferred, rather than the simpler one in Fig. 3c, which has the same composition?" The only obvious difference between them is that the model in Fig. 3c contains junctions between blocks, marked M, which differ from any of those found in Figs. 2, 3a, or, in fact, in the structure of  $\alpha\text{-ZrNb}_{24}\text{O}_{62}$  (Fig. 3d). Junctions of this type contain octahedra which share five of their twelve edges with neigh-

boring octahedra, and they are not common in oxide structures. They have been found in  $(\text{W}_{0.35}\text{V}_{0.65})_2\text{O}_5$  (7),  $(\text{W}_{0.2}\text{V}_{0.8})_3\text{O}_7$  (8) and in the M form of  $\text{Nb}_2\text{O}_5$  (9), but these phases are low-temperature forms, and they transform at about 1200 K to more stable structures, in which the M-type junctions are replaced by others in which octahedra do not share so many edges. On the basis of these observations, it is not surprising that the  $\beta$  and  $\gamma$  polymorphs of  $\text{ZrNb}_{24}\text{O}_{62}$ , which were prepared by heating the  $\alpha$  form at 1640 K, possess structures which are rearranged so as to eliminate M-type junctions. However, we have been unable to find a satisfactory explanation for the metastability of the  $\alpha$ -form (Fig. 3d). It contains the same proportion of tetrahedral sites as the  $\beta$  and  $\gamma$  forms, and the junctions marked X all have the same structure, in which octahedra share a maximum of four edges with their neighbours.

We believe that this work demonstrates the value of high-resolution microscopy particularly well. However, it should be emphasized that the application of the technique to other systems may not necessarily be as successful. We are dealing here with a structure which has a very short projection axis ( $b = 0.38$  nm), with minimum overlap of heavy atoms, and containing empty tunnels within the blocks of octahedra. Also, the

material belongs to a family of phases which have been studied very thoroughly from a structural point of view, and for which a considerable expertise in the recording and interpretation of lattice images has been accumulated. There is no doubt that the technique will be valuable for the study of numerous other systems, but probably only in conjunction with, rather than as a replacement for single crystal X-ray studies. In addition, a great deal remains to be learned about the theoretical aspects of lattice imaging, including the contrast behaviour to be expected from crystals, as a function of thickness and focusing conditions.

### Acknowledgment

One of the authors (S. I.) wishes to thank Professor J. M. Cowley for his continuous encouragement, and to acknowledge the support of a N.S.F. Area Development Grant in Solid State Science (No. GU 3169).

### References

1. J. G. ALLPRESS AND R. S. ROTH, *J. Solid State Chem.* **2**, 366 (1970).
2. R. S. ROTH AND A. D. WADSLEY, *Acta Crystallogr.* **18**, 724 (1965).
3. A. D. WADSLEY AND S. ANDERSSON, in "Perspectives in Structural Chemistry" (J. D. Dunitz and J. A. Ibers, Eds.), Vol. III, John Wiley and Sons, New York (1970).
4. N. C. STEPHENSON, J. P. BEALE, AND D. C. CRAIG, in "Proceedings of 5th Materials Research Symposium" (R. S. Roth and S. J. Schneider, Eds.), National Bureau of Standards Special Publication 364, Solid State Chemistry, National Bureau of Standards, Washington (1972).
5. S. IJIMA, *Acta Crystallogr.* **A29**, 18 (1973).
6. S. IJIMA, *J. Appl. Phys.* **42**, 5891 (1971).
7. M. ISRAELSSON AND L. KIHNBORG, *Arkiv. Kemi* **30**, 129 (1968).
8. J. DARRIET AND J. GALY, *J. Solid State Chem.* **4**, 357 (1972).
9. W. MERTIN, S. ANDERSSON, AND R. GRUEHN, *J. Solid State Chem.* **1**, 419 (1970).